



Article

# TNC and GJA1 Are Putative Progenitor Markers That Are Localized in the Perivascular Adventitia of the Adult Monkey Brain Subventricular Niche

Martin N. Ivanov <sup>1,2,\*</sup> , Dimo S. Stoyanov <sup>1</sup>, Lora V. Veleva <sup>1</sup> , Andon M. Mladenov <sup>1</sup> , Stoyan P. Pavlov <sup>1</sup> , Tetsumori Yamashima <sup>3</sup> and Anton B. Tonchev <sup>1,2,\*</sup>

<sup>1</sup> Department of Anatomy and Cell Biology, Faculty of Medicine, Medical University, 9000 Varna, Bulgaria; dimo.stoyanov@mu-varna.bg (D.S.S.); lora.veleva@mu-varna.bg (L.V.V.); andonmladenov5@gmail.com (A.M.M.); stoyan.pavlov@mu-varna.bg (S.P.P.)

<sup>2</sup> Department of Stem Cell Biology, Research Institute, Medical University, 9000 Varna, Bulgaria

<sup>3</sup> Department of Neurosurgery, Division of Neuroscience, Kanazawa University Graduate School of Medical Science, Kanazawa 920-8641, Japan; yamashima215@gmail.com

\* Correspondence: martin.ivanov@mu-varna.bg (M.N.I.); anton.tonchev@mu-varna.bg (A.B.T.)

**Abstract:** The largest area in the adult mammalian brain that contains stem and progenitor cells at different stages of differentiation is the subventricular zone located along the lateral wall of the lateral ventricle. We have previously shown in adult monkeys that transient global cerebral ischemia upregulates the expression of hundreds of genes in this zone, including genes known to be related to stemness in the rodent brain. Here, we analyzed the immunophenotype of two of these genes, *TNC* and *GJA1*, by co-expression experiments, applying a panel of known stem/progenitor-cell-related markers. We found that both *TNC* and *GJA1* were expressed in the perivascular region. They were localized not to the endothelial cells but to the periendothelial adventitial cells, which was consistent with our previous electron-microscopic data suggesting periendothelial cells as a source of progenitors. We report that the expression of *GJA1* was high in quiescent progenitors, while *TNC* was mostly present in progenitors in the transition from a quiescent to an active state. Our data suggest that *TNC* and *GJA1* can be used as markers for stem/progenitor cells in the largest stem cell area of the adult primate brain.

**Keywords:** *TNC*; *GJA1*; SVZ; neurogenesis; markers



Academic Editor: Francesco Moccia

Received: 25 December 2024

Revised: 23 January 2025

Accepted: 4 February 2025

Published: 7 February 2025

**Citation:** Ivanov, M.N.; Stoyanov, D.S.; Veleva, L.V.; Mladenov, A.M.; Pavlov, S.P.; Yamashima, T.; Tonchev, A.B. *TNC* and *GJA1* Are Putative Progenitor Markers That Are Localized in the Perivascular Adventitia of the Adult Monkey Brain Subventricular Niche. *Int. J. Mol. Sci.* **2025**, *26*, 1397. <https://doi.org/10.3390/ijms26041397>

**Copyright:** © 2025 by the authors. Licensee MDPI, Basel, Switzerland. This article is an open access article distributed under the terms and conditions of the Creative Commons Attribution (CC BY) license (<https://creativecommons.org/licenses/by/4.0/>).

## 1. Introduction

The process by which new neurons are produced by stem/progenitor cells in the adult brain is known as adult neurogenesis. This process occurs in specialized histological domains known as neurogenic niches: the subventricular zone of the lateral ventricle (SVZ) and the subgranular zone (SGZ) of the dentate gyrus [1–3]. The presence of proliferating and differentiating cells in these niches is widely studied in rodents and less studied in primates. The neural stem cells (NSCs) in the brain of mammals exist in different stages of development, such as active NSCs (aNSCs) or quiescent NSCs (qNSCs) [4,5]. Rarely dividing and inactive under physiological conditions, qNSCs can transform into aNSCs after stimulation, and as aNSCs, become highly proliferative and exhibit distinct differences in their immunophenotypic characteristics [6]. In particular, aNSCs begin to express the Epidermal Growth Factor Receptor (EGFR). qNSCs do not express proliferation indicator proteins such as Ki67 (a marker expressed during the G1 phase of the cell cycle) [7]. The investigation of the presence and proliferation of neural stem cells and their progeny in

the adult primate, including humans, brain is slowed down by the lack of reliable markers for these cells [8–12]. Thus, environmental triggers that can stimulate qNSC to adopt an activated state are useful when studying the qNSC-to-aNSC transition. Ischemic stroke is caused by the thromboembolic blockage of a major cerebral blood vessel or one of its branches. The occlusion of a cerebral vessel leads to blood and oxygen deprivation. This condition is an established trigger of increased brain progenitor cell proliferation in primates [13,14]. A public digital database ([www.monkey-niche.org](http://www.monkey-niche.org)) shows the expression changes in 150 genes that accompany the post-ischemic increase in NSC proliferation in the adult primate SVZ [15]. Here, we visually inspected the images of the 150 genes included in the database and selected 2 candidate genes: *TNC* and *GJA1*. We provide evidence suggesting that *TNC* and *GJA1* are candidate genes that mark stem and progenitor cells in the normal adult monkey anterior SVZ (SVZa).

*TNC* (Tenascin-C) is an extracellular protein found around neurons and glia in the CNS and also in stem cell niches in the intestinal crypts, bone marrow, and hair follicles. Its presence has been described in various pathological conditions, namely, tumor masses, inflammation, and mechanical and chemical injuries, with its expression being enhanced during tissue regeneration [16,17]. As part of the extracellular matrix (ECM), *TNC* is directly involved in adhesion to other ECM proteins like fibronectin, integrin, collagen, periostin, fibrillin-2, and others [16,17]. *TNC* has the ability to induce EGFR expression, thus stimulating cell proliferation [18]. *TNC* interacts with factors like TGF $\beta$  (Transforming Growth Factor beta), Wnt3a (Wingless 3a), and VEGF (Vascular Endothelial Growth Factor). *TNC* is known to be expressed in the rodent neurogenic niche, limited to the subependymal layer (SEL) of the SVZ and rostral migratory stream (RMS) [17]. In the rodent SVZ, *TNC* expression was detected in GFAP+ cells, most likely qNSCs, but not in cells expressing markers like PSA-NCAM (Polysialylated —Neural Cell Adhesion Molecule), marking neuroblasts, and *Ascl1* (Achaete-scute homolog 1), marking transit-amplifying progenitor cells (TAPs) [19].

*GJA1* (Connexin 43) is a transmembrane protein that plays a crucial role in intercellular communication. It is expressed in various tissues and organs, including the brain. *GJA1* is expressed in both embryonic and adult subventricular zones, where it plays a role in maintaining the proliferative abilities of NSCs. The elevated expression of *GJA1* is sufficient to stimulate the formation of functional extracellular channels, which is an important condition for maintaining and proliferating NSCs. Additionally, the levels of *GJA1* decrease as NSCs begin to differentiate into neurons [20,21].

Our previous transcriptomic analysis revealed the significant upregulation of *TNC* and *GJA1* in the SVZ following transient global cerebral ischemia. This selective upregulation points to their relevance in the primate SVZ microenvironment and their potential as key markers for progenitor cell identification [15]. Furthermore, we utilized our bioinformatic analysis of the transcriptome data and compared it to available SVZ transcriptomes. When making this comparison with Dulken et al., we found that *GJA1* is enriched in the categories of astrocytes and qNSC-like cells, while *TNC* was enriched within the astrocyte category [7]. When comparing our data with Llorens-Bobadilla et al.'s dataset, we found that *GJA1* was enriched in primed qNSCs [5]. Colorimetric in situ hybridization (ISH) staining showed that these two genes were markedly induced in the subependymal region of the SVZa that hosts the stem progenitor cells in the primate brain [15]. In particular, *TNC* and *GJA1* expression was common in perivascular adventitial cells that represent putative progenitors in the primate SGZ neurogenic niche [22]. In the present study, we performed fluorescent in situ hybridization (FISH) for each of the selected genes followed by the immunohistochemical co-labeling of markers for proliferation and known cell types in order to probe the putative expression of *TNC* and *GJA1* in stem/progenitor cells in intact monkey

brains. We studied the expression of these genes before and after cerebral ischemia, which is known to induce SVZ progenitor cell proliferation, and combined these expression studies with immunolabeling for known markers of brain cell types. Our selection of *TNC* and *GJA1* as candidate markers for neural stem/progenitor cells in the primate SVZ is supported by their distinct functional roles, spatial localization, and relevance to neurogenic processes. By highlighting these markers' specific contributions to identifying and characterizing progenitor populations, we aim to advance the understanding of stem cell biology in the adult primate brain and bridge interspecies differences in neurogenesis research. Our results demonstrate that a combinatorial labeling strategy may prove an effective method in the visualization of neural stem/progenitor cells in the adult primate brain.

## 2. Results

### 2.1. *TNC* and *GJA1* Expression in the SVZa Before or After Cerebral Ischemia

Utilizing a publicly available database ([www.monkey-niche.org](http://www.monkey-niche.org) accessed on 18 February 2024) of gene expression before or after brain ischemia in the adult monkey SVZ, we noticed that *TNC* and *GJA1* were markedly increased after ischemia in the subependymal region that hosts the stem/progenitor cells in the primate brain [15]. Moreover, the selected two genes also demonstrated a marked increase in expression with a distinct clustering of the cells in the SVZ and, more notably, perivascularly (Figure 1), which is characteristic of progenitors [22]. It should be noted that the endothelial cells on the SVZ blood vessels (BVs) did not seem to be positive for either *TNC* or *GJA1*.

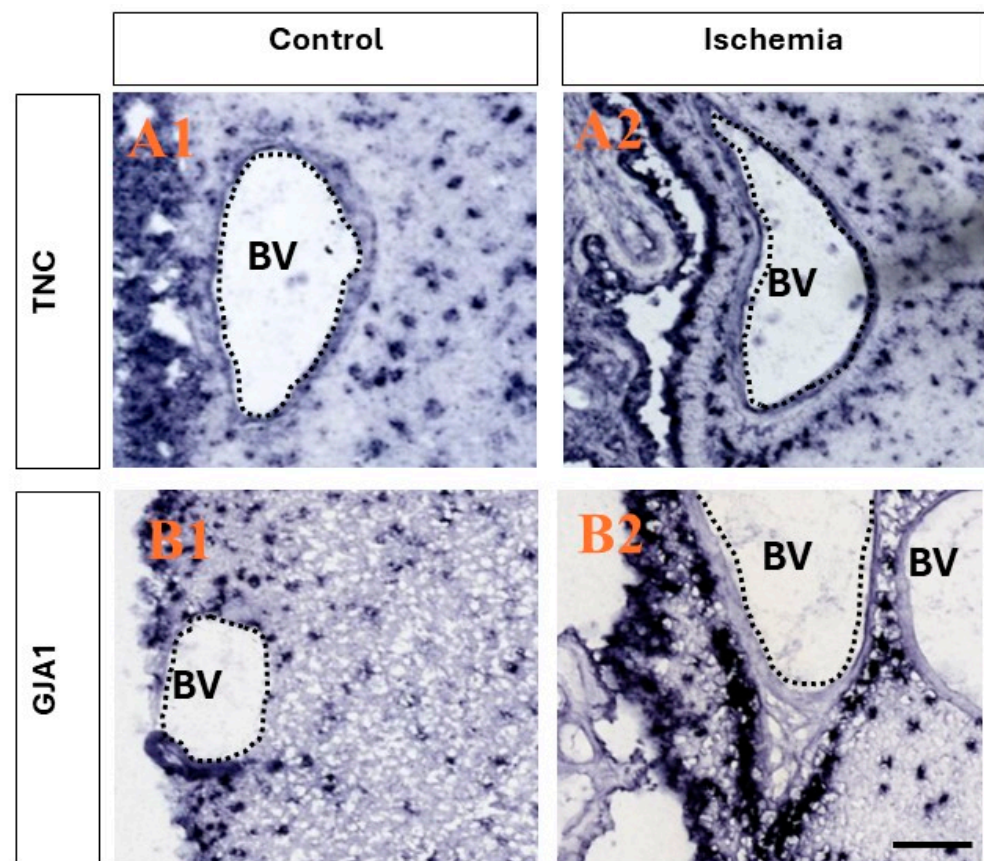


**Figure 1.** Ischemia-induced upregulation of the expression of *TNC* and *GJA1* in adult monkey neurogenic niche. (A1,A2) Comparison between the expression of *TNC* before and after ischemia. After ischemia, a stronger presence is seen in both the ependymal layers and in the SVZ, and the clustering of positive *TNC*+ cells is observed in close association with the blood vessels in the region,



while little to no expression is seen in the epithelial cells lining the blood vessels. **(B1,B2)** Comparison between the expression of *GJA1* before and after ischemia. After ischemic injury, an increase in expression in the ependymal layers and SVZ is observed, and intense staining is observed in close association with the blood vessels, with no staining in the epithelial cells lining the blood vessels. Images derived from [www.monkey-niche.org](http://www.monkey-niche.org). Scale bar—200  $\mu$ m. BV—blood vessel.

## 2.2. Immunophenotype of TNC-Expressing Cells

Immunohistochemical staining for GFAP, VIM, and BrdU was conducted in combination with FISH for *TNC*. First, we calculated the fraction of double-positive (*TNC*+/*marker*+) cells of all SVZ cells (marked by DAPI). Our staining showed that *TNC*+/*GFAP*+ cells and *TNC*+/*VIM*+ cells represented approximately a quarter of the cells in the SVZa, while *TNC*+/*BrdU*+ were only 1.4% of the cells in the SVZa.

We studied the fraction of *GFAP*+ cells expressing *TNC*. *GFAP* is a marker for qNSC/parenchymal astrocytes [4,7]. We discovered that while two-thirds of the *GFAP*+ cells co-expressed *TNC* (95% CI 60.45–74.42%), only one-third of the *TNC*+ cells were co-labeled for *GFAP* (95% CI 28.15–37.87%) (a total of 1158 counted cells) (Figure 2). We also studied the fraction of *VIM*+ cells that were co-labeled for *TNC*. *VIM* is a marker for aNSCs, TAPs, and blood vessels [15]. We found that 27% of the *TNC*+ cells were positive for *VIM* (95% CI 29.96–43.52%), while 81% of the *VIM*+ cells expressed *TNC* (95% CI 74.45–90.42%) (a total of 716 counted cells). To track and quantify de novo generated cells in this area, we injected monkeys with BrdU [13,14] followed by immunostaining. Double-labeling *TNC*/BrdU experiments showed that 3% of all *TNC*+ cells were BrdU-positive (95% CI 1.67–3.61%), while 56% of all BrdU+ cells were *TNC*-positive (95% CI 43.52–71.93%) (a total of 4244 counted cells). To differentiate between qNSCs and aNSCs, we used triple staining, including *GFAP* and BrdU in combination with *TNC*. This revealed the existence of a subpopulation of *TNC*+/*GFAP*+/*BrdU*+, 1.3% of all DAPI+ cells, representing NSCs initiating proliferation (Figure 2(D4)). In contrast, the non-proliferative (quiescent) qNSC fraction (*TNC*+/*GFAP*+/*BrdU*−) was estimated to be 21.4% of all SVZa cells (Figure 2(D4)).

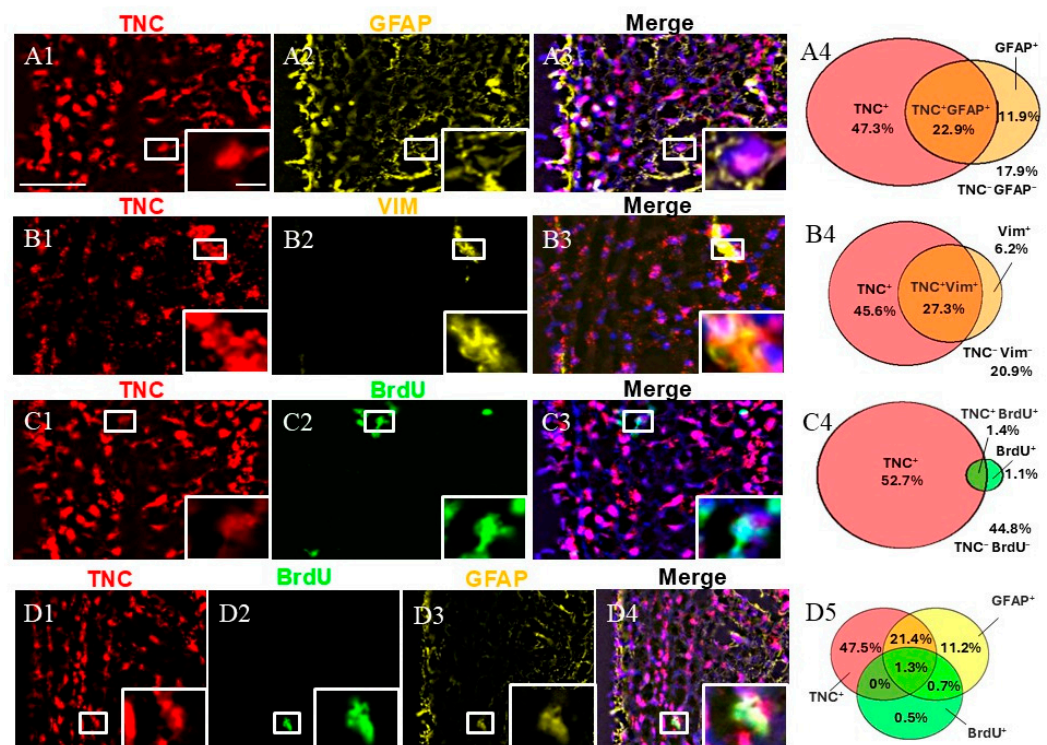


**Figure 2.** Expression pattern of *TNC*+ cells in adult monkey SVZa. **(A1–A3)** Dual staining for *TNC* (red) and *GFAP* (yellow) counterstained with DAPI. *TNC*/*GFAP* co-staining demonstrates the

presence of *TNC*+/*GFAP*+ cells (insert). **(B1–B3)** Dual staining for *TNC* (red) and *VIM* (yellow). *TNC*/*VIM* co-staining reveals the presence of *TNC*+/*VIM*+ cells (insert). **(C1–C3)** Dual staining for *TNC* (red) and *BrdU* (green). *TNC*/*VIM* co-staining shows the presence of *TNC*+/*BrdU*+ cells (insert). **(D1–D4)** Triple staining for *TNC* (red), *GFAP* (yellow), and *BrdU* (green) demonstrates the presence of the proliferative NSCs (*TNC*+/*GFAP*+/*BrdU*+; insert). **(A4,B4,C4,D5)** Venn diagrams depicting the share of different cell subpopulations. The percentages reflect the fraction of a specific cellular expression pattern of all cells in the SVZ as stained by DAPI. Scale bar—100  $\mu$ m. Scale bar insert—20  $\mu$ m.

### 2.3. Immunophenotype of *GJA1*-Expressing Cells

An immunophenotypic analysis of *GJA1*+ cells was performed using the markers *GFAP*, *VIM*, and *BrdU* (Figure 3). Dual labeling revealed that while *GJA1*+/*GFAP*+ represented approximately a quarter of the SVZ cells (Figure 3(A4)), *GJA1*+/*VIM*+ and *GJA1*+/*BrdU*+ were less than 10% of the SVZ cells (Figure 3(B4,C4)).

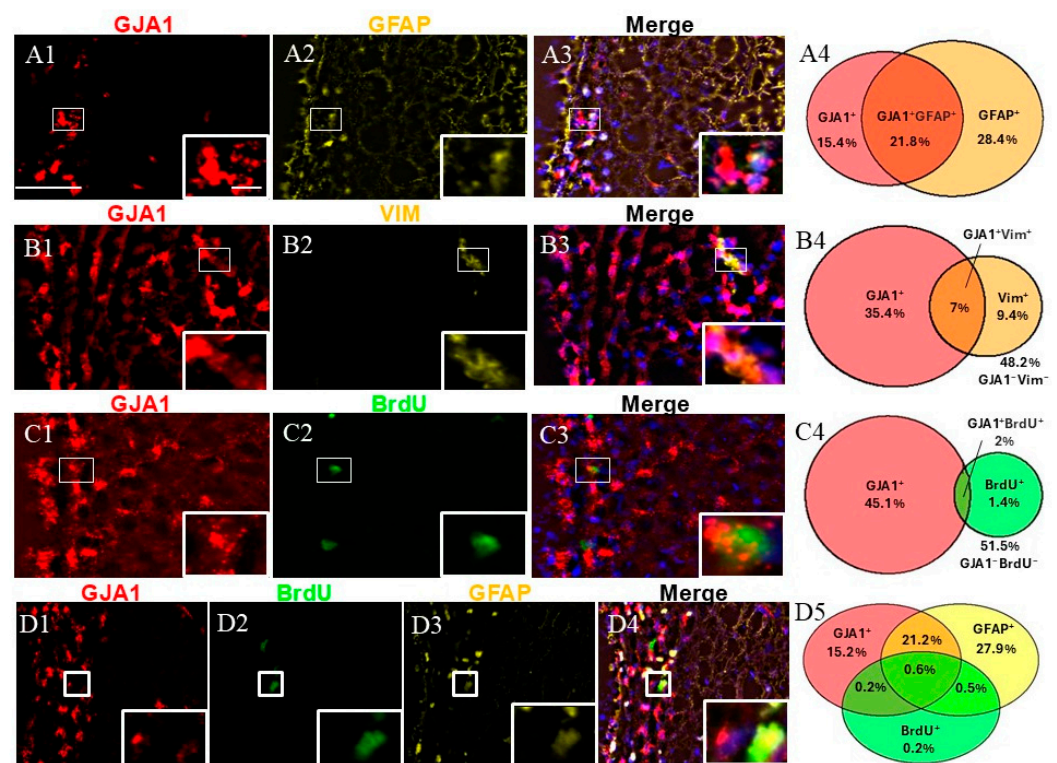


**Figure 3.** Cell identity of *GJA1*+ cells in adult monkey rostral SVZ. **(A1–A3)** Dual staining for *GJA1* (red) and *GFAP* (yellow). *GJA1*/*GFAP* co-staining demonstrates the presence of *GJA1*+/*GFAP*+ cells (insert). **(B1–B3)** Dual staining for *GJA1* (red) and *VIM* (yellow) reveals the presence of *GJA1*+/*VIM*+ cells (insert). **(C1–C3)** Dual staining for *GJA1* (red) and *BrdU* (green). *GJA1*/*BrdU* co-staining reveals the presence of proliferative cells *GJA1*+/*BrdU*+ (insert). **(D1–D4)** Triple staining for *GJA1* (red), *GFAP* (yellow), and *BrdU* (green). *GJA1*/*GFAP*/*BrdU* co-staining demonstrates the presence of proliferative NSCs (*GJA1*+/*GFAP*+/*BrdU*+, insert). **(A4,B4,C4,D5)** Venn diagrams depicting the different cell subpopulations. The percentages reflect the fraction of a specific cellular expression pattern of all cells in the SVZ as stained by DAPI. Scale bar—100  $\mu$ m. Scale bar insert—20  $\mu$ m.

We studied the fraction of *GFAP*+ cells expressing *GJA1*. More than half of the *GJA1*+ fraction co-expressed *GFAP* (95% confidence interval: 45.92–60.64%), and again, nearly half of the *GFAP*+ cells co-expressed *GJA1* (95% confidence interval: 34.26–47.04%) (a total of 1033 counted cells). The evaluation of *GJA1*/*VIM* showed that 16.4% of all *GJA1*+ cells co-expressed *VIM* (95% confidence interval: 14.01–20.60%), and nearly half (42%)

of the VIM+ cells co-expressed *GJA1* (95% confidence interval: 33.40–53.78%) (a total of 1250 counted cells). Additionally, 4% of all BrdU+ cells co-expressed *GJA1* (95% confidence interval: 2.46–5.72), whereas more than half (57.6%) of all *GJA1*+ cells co-expressed BrdU (95% confidence interval: 43.33–73.52%) (a total of 2717 counted cells). Finally, when we evaluated a triple combination of BrdU, GFAP, and *GJA1*, our results revealed that 0.6% of all cells were triple-positive (*GJA1*+ / GFAP+ / BrdU+), representing NSCs in a proliferative state, while 21.1% of the cells were *GJA1*+ / GFAP+ / BrdU−, thus representing a quiescent state (a total of 1033 counted cells).

#### 2.4. Dual Labeling for TNC and *GJA1*

Next, we investigated the cells expressing both TNC and *GJA1* (Figure 4). To this end, we utilized dual FISH staining for TNC and *GJA1* and found that 27.2% of all studied SVZ cells were TNC+/*GJA1*+, while 21.3% were TNC+/*GJA1*− and 16.5% were TNC−/*GJA1*+ (Figure 4(A1–A4)) (a total of 2540 counted cells). To investigate deeper the expression pattern of these cell subpopulations, we combined TNC/*GJA1* dual FISH with immunohistochemical staining for BrdU or VIM (Figure 4(B1–C5)). We discovered that triple-positive TNC+/*GJA1*+ / BrdU+ cells represented a very small (~1%) fraction of the SVZ cells (Figure 4(B5)) (a total of 1041 counted cells), while the TNC+/*GJA1*+ / VIM+ cells accounted for 7–8% of the SVZ cells (Figure 4(C5)) (a total of 716 counted cells). Interestingly, we noticed the presence of a significant subpopulation of SVZ cells that were *GJA1*+ / TNC− (~25% of the SVZ cells), and these cells expressed neither BrdU (Figure 4(B5)) nor VIM (Figure 4(C5)).

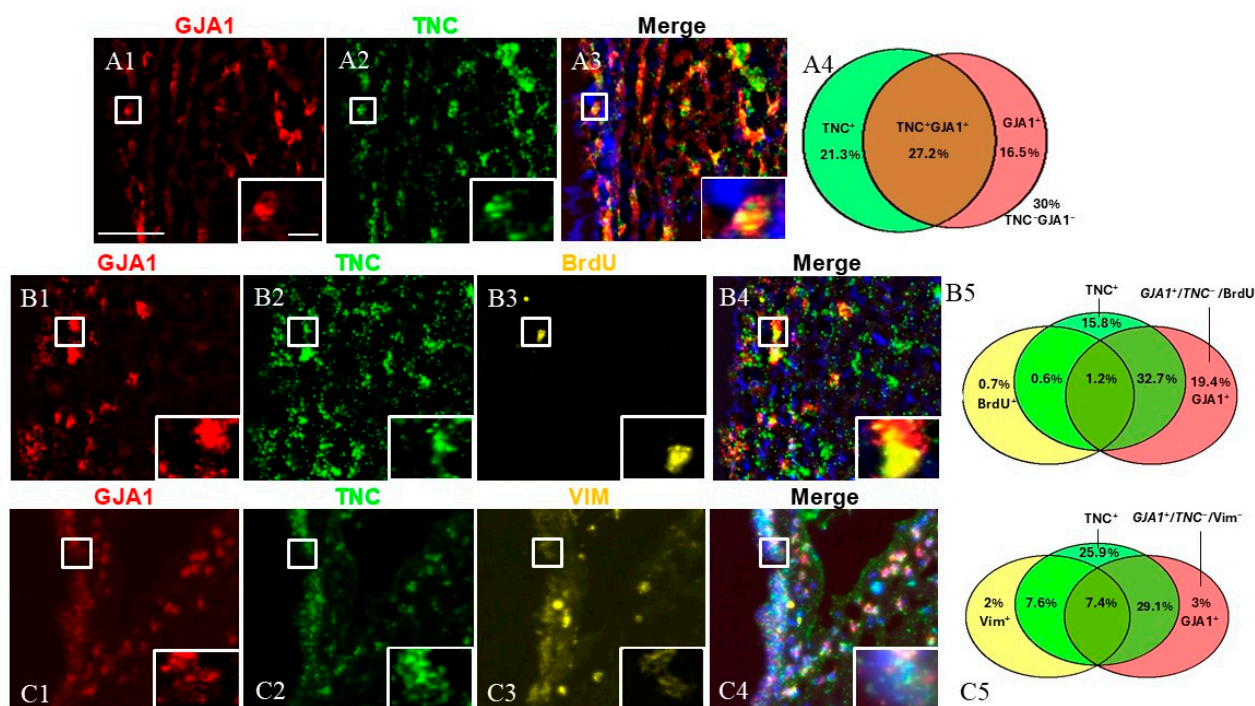


**Figure 4.** SVZa cell subpopulations expressing TNC and *GJA1*. (A1–A3) Dual FISH staining for TNC (green) and *GJA1* (red). A TNC+/*GJA1*+ cell is shown in the insert. (B1–B4) Dual FISH staining for TNC (green) and *GJA1* (red) in combination with BrdU (yellow) demonstrates the presence of a *GJA1*+ / TNC− / BrdU− population (C1–C4). Dual FISH staining for TNC (green) and *GJA1* (red) in combination with VIM (yellow) demonstrates the presence of a *GJA1*+ / TNC− / VIM− population (insert). (A4,B5,C5) Venn diagrams depicting the different cell subpopulations. The percentages reflect the fraction of a specific cellular pattern of all SVZa cells (stained by DAPI). Scale bar: 100  $\mu$ m. Scale bar insert: 20  $\mu$ m.



### 3. Discussion

The level of neurogenesis varies among species, with it being lower in primates compared to the commonly used rodent models [23]. Furthermore, research on adult neurogenesis in non-human primates offers limitations due to technological and ethical constraints [24–26]. Of note, the structural organization of the NSC niche shows interspecies differences between rodents and primates [27]. Thus, the identification of markers of progenitor cell populations in the stem cell niche of primates is of pivotal importance in tracking these cells and being able to identify them in their complex environment in the niche [28,29].

Aging is a critical factor influencing neurogenesis and the expression of key markers in the primate SVZ. Studies have shown that *TNC* expression decreases with age in tissues such as skin, cartilage, and the cardiovascular system. This downregulation is linked to reduced regenerative capacity and extracellular matrix remodeling in conditions like fibrosis and cardiovascular diseases [30,31]. This response may exacerbate maladaptive remodeling and inflammation. Aging is also associated with decreased *GJA1* expression in many tissues, impairing gap-junction-mediated communication [32]. Aging impacts the phosphorylation, localization, and turnover of *GJA1*, reducing its effectiveness [33]. Age-related oxidative stress and inflammation exacerbate *GJA1* dysfunction, particularly in the nervous system [34].

In addition to the expression of *TNC* and *GJA1*, various signaling pathways, such as BMP, WNT, and NOTCH, are critical in regulating neurogenesis and progenitor cell behavior in the adult brain, particularly in response to injury or aging [35,36]. NOTCH signaling, known for maintaining progenitor cell quiescence, likely plays a role in regulating the activation of cells expressing *TNC* and *GJA1* [37]. BMP signaling, which is involved in cell differentiation and repair, might modulate the transition of progenitors from quiescence to an active state [38]. Meanwhile, WNT signaling is crucial for progenitor cell proliferation and migration, which could be particularly relevant in ischemic injury models where tissue regeneration is required [39]. The interactions between these pathways, particularly in the context of *TNC* and *GJA1* expression, might dictate the behavior of progenitor cells and their response to injury, including ischemia.

Further studies exploring how these pathways interact with *TNC* and *GJA1* in the primate SVZ will be important to understand how cellular behaviors such as activation, proliferation, and differentiation are regulated in the stem cell niche of primates.

Here, we report for the first time the cellular immunophenotypic characteristics of cells expressing *TNC* and *GJA1* in the adult primate SVZ. Our findings show that in the normal adult monkey SVZ, *TNC* and *GJA1* are expressed by both qNSCs and aNSCs. Our combined FISH/immunofluorescent analyses revealed two subpopulations of *TNC*<sup>+</sup> cells: GFAP<sup>+</sup>/*TNC*<sup>+</sup>/BrdU<sup>−</sup> (putative qNSCs) and GFAP<sup>+</sup>/*TNC*<sup>+</sup>/BrdU<sup>+</sup> (putative aNSCs). Thus, while *TNC* is expressed by stem cells in both rodents and monkeys, in monkeys, *TNC* is also expressed by the aNSC/TAP (*TNC*<sup>+</sup>/VIM<sup>+</sup>) population of progenitors. In the rodent SVZ, *TNC* expression is restricted to GFAP<sup>+</sup> cells [19], and thus, our data showing that *TNC* expression is maintained in a primate aNSC/TAP population suggest an interspecies difference.

Similarly to *TNC*, we detected two subpopulations of *GJA1*<sup>+</sup> cells: GFAP<sup>+</sup>/*GJA1*<sup>+</sup>/BrdU<sup>−</sup> (putative qNSCs) and GFAP<sup>+</sup>/*GJA1*<sup>+</sup>/BrdU<sup>+</sup> (putative aNSCs). *GJA1* has a role in maintaining the proliferation and self-renewal of NSCs in mice. This is in line with our data, which may represent an interspecies similarity in the stem cell biology of the SVZ. We also observed a distinct decrease in gene expression when cells gradually differentiated from qNSCs to aNSCs in the two examined genes.

Additionally, using co-staining with *TNC* and *GJA1*, we discovered a subpopulation of *GJA1*<sup>+</sup>/*TNC*<sup>−</sup> cells, which was negative for both VIM and BrdU (Figure 4). The *GJA1*<sup>+</sup>/*TNC*<sup>−</sup> expression pattern most likely corresponds to a quiescent progenitor or to niche astrocytes.

A present limitation in brain stem cell research is the fact that the currently used markers can label more than one type of cellular subpopulation. For example, GFAP can label both qNSCs and niche astrocytes. Similarly, VIM and BrdU can label more than one cell population. In the current study, we chose a different starting point when focusing on the genes of interest: we used cerebral ischemia as a tool to trigger stem cell activation, and, at the same time, we searched for genes with a specific perivascular expression pattern, as such a pattern was proved to label progenitors in the hippocampal niche [22]. Furthermore, we employed a triple-labeling combining FISH with dual immunofluorescence approach to combine the gene of interest with the expression of not one but two different markers, in combinations. This combinatorial labeling allowed us to distinguish between qNSCs (GFAP<sup>+</sup>/VIM<sup>−</sup>/BrdU<sup>−</sup>) or aNSCs (GFAP<sup>−</sup>/VIM<sup>+</sup>/BrdU<sup>+</sup>) and define the fractions of these progenitors that express *TNC* and *GJA1*. An important step in differentiating qNSCs from niche astrocytes emerged from our effort to better characterize the molecular features of *TNC*<sup>−</sup> and *GJA1*<sup>−</sup> expressing cells. One putative fraction representing the niche astrocytes is the population of *GJA1*<sup>+</sup>/*TNC*<sup>−</sup> cells that we observed. Future research may clarify the molecular mechanisms by which cerebral ischemia regulates the expression of *TNC* and *GJA1*.

#### 4. Materials and Methods

For our experiments, we used tissues from 4 adult (four–six years old at the time of the experiment) macaque monkeys (*Macaca fuscata*). The tissues were derived following an experimental procedure approved by the Animal Care and Ethics Committee of Kanazawa University, Japan (approval protocols #AP-031498 and #AP-080920). Ischemia was induced using surgical procedures described previously [13,14]. To induce global ischemia, each monkey was anesthetized (ketamine at a dose of 2–5 mg/kg, i.m.), intubated, and connected to a ventilator. During the surgical procedures, the monkeys were additionally anesthetized via inhalation (1% halothane, gas mixture 40% O<sub>2</sub>/60% N<sub>2</sub>O). Arterial blood pressure, pulse, pupil diameter, and response were monitored. During the operation, the animals' body temperature was maintained within 37 ± 0.5 °C. The surgical procedure for global ischemia was performed under sterile conditions in the following sequence: anterior median thoracotomy, the dissection of the skin and subcutaneous tissue, sternotomy, the dissection of soft tissues, and the visualization of the left subclavian artery and brachiocephalic trunk. One of the four monkeys received 5-bromo-2'-deoxyuridine (BrdU 100 mg/kg, i.v., from Sigma-Aldrich Corp., St. Louis, MO, USA) for 5 days and was sacrificed 2 h after the last BrdU application. Coronal sections of the anterior subventricular zone (SVZa) were cut on a freezing microtome (Leica CM3050 S, Leica Biosystems, Deer Park, IL, USA) at 20 micrometers. The non-radioactive in situ hybridization (ISH) staining procedure and the combinatorial labeling protocol with cell type markers have been published previously [15]. Briefly, macaque monkey-specific templates, 600–900 nucleotides long, were synthesized using RNA isolation, cDNA synthesis, and PCR amplification. The templates were generated using the following specific primers—*TNC* Forward: CAGAG-GAAGGAGCTCGCTA; *TNC* Reverse: GACACCAGGTTCTCCAGCTC; *GJA1* Forward: AGCCTACTCAACTGCTGGAG; and *GJA1* Reverse: TCGCCAGTAACCAGCTTGTA. The primer and template sequences used for the ISH of the genes *TNC* and *GJA1* were identical to those published at [www.monkey-niche.org](http://www.monkey-niche.org) [20]. In vitro transcription was used to generate Digoxigenin-tagged riboprobes. Hybridized probes were identified using a



two-step chromogenic catalyzed reporter deposition method. For FISH staining, the *TNC* and *GJA1* hybridized probe was detected with fluorochrome-labeled reagents. Following fluorescent ISH (FISH), sections were subjected to antigen retrieval (Dako PT Link, Agilent Technologies, Santa Clara, CA, USA) with a citrate buffer (pH 6) and blocked with Bovine serum albumin diluted 1:10 in 1% of Triton X-100/PBS. We used the following primary antibodies: anti-BrdU (1:100, Cat. No Ab6326, Abcam, Cambridge, UK), anti-GFAP (1:400 Cat. No M0761, Dako-Agilent Technologies GmbH, Hamburg, Germany), anti-GFAP (1:1000, Cat. No AB5541, Merck Millipore, Burlington, MA, USA), and anti-VIM (1:1000, Cat. No MAB3400, Merck Millipore, Burlington, MA, USA). The primary antibodies were visualized by species-specific secondary antibodies, counterstained with DAPI and covered with mountant media (Invitrogen™ ProLong™ Gold Antifade Mountant, Thermo Fisher Scientific, Waltham, MA, USA). A high-resolution mosaic image of the periventricular tissues was captured using an EC Plan-Neofluar 20×/0.50 objective with a lateral resolution of 0.65 μm/px. These images serve as a reference database and are intended for future analyses. A series of 3 to 5 z-stacks per microscope slide were obtained from the SVZ using an EC Plan-Neofluar 40×/0.75 objective, with a lateral resolution of 0.325 μm/px and an axial resolution (z-distance) ranging from 0.125 to 0.55 μm. The camera was set to a binning factor of 2 × 2 to reduce both scanning time and camera noise. The z-stacks from the striatal SVZ were captured sequentially, starting from the dorsolateral edge of the ventricle and progressing medially. The co-localization quantification of cells labeled by fluorescent immunohistochemistry was conducted as described previously [15]. Briefly, using a semi-automated digital workflow, we processed the acquired images by channel extraction and denoising followed by the top-hat filtering, channel thresholding, classification, and counting of the cell in a region of interest (1000 cells per specimen).

**Author Contributions:** Conceptualization, M.N.I. and A.B.T.; methodology, M.N.I. and A.B.T.; investigation, M.N.I., D.S.S., L.V.V., A.M.M. and S.P.P.; resources, M.N.I., A.B.T. and T.Y.; writing—original draft preparation, M.N.I. and A.B.T.; writing—review and editing, M.N.I., A.B.T. and T.Y.; visualization, M.N.I.; supervision, A.B.T.; funding acquisition, M.N.I. and A.B.T. All authors have read and agreed to the published version of the manuscript.

**Funding:** This research was funded by an intramural grant of the Medical University-Varna (21020/2021) (M.N.I. and A.B.T) and The European Commission Horizon 2020 Framework Program (Project 856871—TRANSTEM) (A.B.T).

**Institutional Review Board Statement:** The animal study protocol was approved by the Institutional Animal Care and Ethics Committee of Kanazawa University, Japan (protocol codes AP-031498 and AP-080920).

**Informed Consent Statement:** Not applicable.

**Data Availability Statement:** All data are contained within the article.

**Acknowledgments:** We are grateful for the technical assistance of Velina Kenovska.

**Conflicts of Interest:** The authors declare no conflicts of interest.

## References

1. Ming, G.-L.; Song, H. Adult Neurogenesis in the Mammalian Brain: Significant Answers and Significant Questions. *Neuron* **2011**, *70*, 687–702. [\[CrossRef\]](#)
2. Bond, A.M.; Ming, G.L.; Song, H. Adult Mammalian Neural Stem Cells and Neurogenesis: Five Decades Later. *Cell Stem Cell* **2015**, *17*, 385–395. [\[CrossRef\]](#) [\[PubMed\]](#)
3. Li, Y.; Guo, W. Neural Stem Cell Niche and Adult Neurogenesis. *Neuroscientist* **2021**, *27*, 235–245. [\[CrossRef\]](#) [\[PubMed\]](#)
4. Codega, P.; Silva-Vargas, V.; Paul, A.; Maldonado-Soto, A.R.; Deleo, A.M.; Pastrana, E.; Doetsch, F. Prospective Identification and Purification of Quiescent Adult Neural Stem Cells from Their In Vivo Niche. *Neuron* **2014**, *82*, 545–559. [\[CrossRef\]](#) [\[PubMed\]](#)

5. Llorens-Bobadilla, E.; Zhao, S.; Baser, A.; Saiz-Castro, G.; Zwadlo, K.; Martin-Villalba, A. Single-Cell Transcriptomics Reveals a Population of Dormant Neural Stem Cells That Become Activated upon Brain Injury. *Cell Stem Cell* **2015**, *17*, 329–340. [[CrossRef](#)] [[PubMed](#)]
6. Chaker, Z.; Codega, P.; Doetsch, F. A Mosaic World: Puzzles Revealed by Adult Neural Stem Cell Heterogeneity. *Wiley Interdiscip. Rev. Dev. Biol.* **2016**, *5*, 640–658. [[CrossRef](#)]
7. Dulken, B.W.; Leeman, D.S.; Boutet, S.C.; Hebestreit, K.; Brunet, A. Single-Cell Transcriptomic Analysis Defines Heterogeneity and Transcriptional Dynamics in the Adult Neural Stem Cell Lineage. *Cell Rep.* **2017**, *18*, 777–790. [[CrossRef](#)]
8. Flor-García, M.; Terreros-Roncal, J.; Moreno-Jiménez, E.P.; Ávila, J.; Rábano, A.; Llorens-Martín, M. Unraveling Human Adult Hippocampal Neurogenesis. *Nat. Protoc.* **2020**, *15*, 668–693. [[CrossRef](#)]
9. Liu, Y.W.J.; Curtis, M.A.; Gibbons, H.M.; Mee, E.W.; Bergin, P.S.; Teoh, H.H.; Connor, B.; Dragunow, M.; Faull, R.L.M. Doublecortin Expression in the Normal and Epileptic Adult Human Brain. *Eur. J. Neurosci.* **2008**, *28*, 2254–2265. [[CrossRef](#)] [[PubMed](#)]
10. Moreno-Jiménez, E.P.; Terreros-Roncal, J.; Flor-García, M.; Rábano, A.; Llorens-Martín, M. Evidences for Adult Hippocampal Neurogenesis in Humans. *J. Neurosci.* **2021**, *41*, 2541–2553. [[CrossRef](#)] [[PubMed](#)]
11. Verwer, R.W.H.; Sluiter, A.A.; Balesar, R.A.; Baayen, J.C.; Noske, D.P.; Dirven, C.M.F.; Wouda, J.; Van Dam, A.M.; Lucassen, P.J.; Swaab, D.F. Mature Astrocytes in the Adult Human Neocortex Express the Early Neuronal Marker Doublecortin. *Brain* **2007**, *130*, 3321–3335. [[CrossRef](#)] [[PubMed](#)]
12. Zwirner, J.; Lier, J.; Franke, H.; Hammer, N.; Matschke, J.; Trautz, F.; Tse, R.; Ondruschka, B. GFAP Positivity in Neurons Following Traumatic Brain Injuries. *Int. J. Legal Med.* **2021**, *135*, 2323–2333. [[CrossRef](#)] [[PubMed](#)]
13. Tonchev, A.B.; Yamashima, T.; Zhao, L.; Okano, H.J.; Okano, H. Proliferation of Neural and Neuronal Progenitors after Global Brain Ischemia in Young Adult Macaque Monkeys. *Mol. Cell. Neurosci.* **2003**, *23*, 292–301. [[CrossRef](#)]
14. Tonchev, A.B.; Yamashima, T.; Sawamoto, K.; Okano, H. Enhanced Proliferation of Progenitor Cells in the Subventricular Zone and Limited Neuronal Production in the Striatum and Neocortex of Adult Macaque Monkeys after Global Cerebral Ischemia. *J. Neurosci. Res.* **2005**, *81*, 776–788. [[CrossRef](#)]
15. Chongtham, M.C.; Wang, H.; Thaller, C.; Hsiao, N.-H.; Vachkov, I.H.; Pavlov, S.P.; Williamson, L.H.; Yamashima, T.; Stoykova, A.; Yan, J.; et al. Transcriptome Response and Spatial Pattern of Gene Expression in the Primate Subventricular Zone Neurogenic Niche After Cerebral Ischemia. *Front. Cell Dev. Biol.* **2020**, *8*, 584314. [[CrossRef](#)] [[PubMed](#)]
16. Midwood, K.S.; Chiquet, M.; Tucker, R.P.; Orend, G. Tenascin-C at a Glance. *J. Cell Sci.* **2016**, *129*, 4321–4327. [[CrossRef](#)]
17. Tucić, M.; Stamenković, V.; Andjus, P. The Extracellular Matrix Glycoprotein Tenascin C and Adult Neurogenesis. *Front. Cell Dev. Biol.* **2021**, *9*, 674199. [[CrossRef](#)] [[PubMed](#)]
18. Garcion, E.; Halilagic, A.; Faissner, A.; French-Constant, C. Generation of an Environmental Niche for Neural Stem Cell Development by the Extracellular Matrix Molecule Tenascin C. *Development* **2004**, *131*, 3423–3432. [[CrossRef](#)] [[PubMed](#)]
19. Kazanis, I.; Belhadi, A.; Faissner, A.; French-Constant, C. The Adult Mouse Subependymal Zone Regenerates Efficiently in the Absence of Tenascin-C. *J. Neurosci.* **2007**, *27*, 13991–13996. [[CrossRef](#)]
20. Cheng, A.; Tang, H.; Cai, J.; Zhu, M.; Zhang, X.; Rao, M.; Mattson, M.P. Gap Junctional Communication Is Required to Maintain Mouse Cortical Neural Progenitor Cells in a Proliferative State. *Dev. Biol.* **2004**, *272*, 203–216. [[CrossRef](#)] [[PubMed](#)]
21. Duval, N.; Gomès, D.; Calaora, V.; Calabrese, A.; Meda, P.; Bruzzone, R. Nathalie Duval Cell Coupling and Cx43 Expression in Embryonic Mouse Neural Progenitor Cells. *J. Cell Sci.* **2002**, *115*, 3241–3251. [[CrossRef](#)] [[PubMed](#)]
22. Yamashima, T.; Tonchev, A.B.; Vachkov, I.H.; Popivanova, B.K.; Seki, T.; Sawamoto, K.; Okano, H. Vascular Adventitia Generates Neuronal Progenitors in the Monkey Hippocampus after Ischemia. *Hippocampus* **2004**, *14*, 861–875. [[CrossRef](#)] [[PubMed](#)]
23. Alunni, A.; Bally-Cuif, L. A Comparative View of Regenerative Neurogenesis in Vertebrates. *Dev. Camb.* **2016**, *143*, 741–753. [[CrossRef](#)]
24. Bonfanti, L.; Peretto, P. Adult Neurogenesis in Mammals—A Theme with Many Variations. *Eur. J. Neurosci.* **2011**, *34*, 930–950. [[CrossRef](#)]
25. Shook, B.A.; Manz, D.H.; Peters, J.J.; Kang, S.; Conover, J.C. Spatiotemporal Changes to the Subventricular Zone Stem Cell Pool through Aging. *J. Neurosci.* **2012**, *32*, 6947–6956. [[CrossRef](#)]
26. Sorrells, S.F.; Paredes, M.F.; Zhang, Z.; Kang, G.; Pastor-Alonso, O.; Biagiotti, S.; Page, C.E.; Sandoval, K.; Knox, A.; Connolly, A.; et al. Positive Controls in Adults and Children Support That Very Few, If Any, New Neurons Are Born in the Adult Human Hippocampus. *J. Neurosci.* **2021**, *41*, 2554–2565. [[CrossRef](#)] [[PubMed](#)]
27. Quiñones-Hinojosa, A.; Sanai, N.; Gonzalez-Perez, O.; Garcia-Verdugo, J.M. The Human Brain Subventricular Zone: Stem Cells in This Niche and Its Organization. *Neurosurg. Clin. N. Am.* **2007**, *18*, 15–20. [[CrossRef](#)] [[PubMed](#)]
28. Donega, V.; van der Geest, A.T.; Sluijs, J.A.; van Dijk, R.E.; Wang, C.C.; Basak, O.; Pasterkamp, R.J.; Hol, E.M. Single-Cell Profiling of Human Subventricular Zone Progenitors Identifies SFRP1 as a Target to Re-Activate Progenitors. *Nat. Commun.* **2022**, *13*, 1036. [[CrossRef](#)]

29. Beckervordersandforth, R.; Tripathi, P.; Ninkovic, J.; Bayam, E.; Lepier, A.; Stempfhuber, B.; Kirchhoff, F.; Hirrlinger, J.; Haslinger, A.; Lie, D.C.; et al. In Vivo Fate Mapping and Expression Analysis Reveals Molecular Hallmarks of Prospectively Isolated Adult Neural Stem Cells. *Cell Stem Cell* **2010**, *7*, 744–758. [[CrossRef](#)] [[PubMed](#)]
30. Park, J.S.; Lee, Y.H.; Lee, D.H.; Chung, J.H.; Lee, S.-T. Expression of Tenascin-C Is down-Regulated during Intrinsic Skin Aging. *J. Dermatol. Sci.* **2017**, *86*, e92–e93. [[CrossRef](#)]
31. Bhattacharyya, S.; Wang, W.; Morales-Nebreda, L.; Feng, G.; Wu, M.; Zhou, X.; Lafyatis, R.; Lee, J.; Hinchcliff, M.; Feghali-Bostwick, C.; et al. Tenascin-C Drives Persistence of Organ Fibrosis. *Nat. Commun.* **2016**, *7*, 11703. [[CrossRef](#)] [[PubMed](#)]
32. Yeh, H.-I.; Chang, H.-M.; Lu, W.-W.; Lee, Y.-N.; Ko, Y.-S.; Severs, N.J.; Tsai, C.-H. Age-Related Alteration of Gap Junction Distribution and Connexin Expression in Rat Aortic Endothelium. *J. Histochem. Cytochem.* **2000**, *48*, 1377–1389. [[CrossRef](#)]
33. Jansen, J.A.; Van Veen, T.A.B.; De Jong, S.; Van Der Nagel, R.; Van Stuijvenberg, L.; Driessen, H.; Labzowski, R.; Oefner, C.M.; Bosch, A.A.; Nguyen, T.Q.; et al. Reduced Cx43 Expression Triggers Increased Fibrosis Due to Enhanced Fibroblast Activity. *Circ. Arrhythmia Electrophysiol.* **2012**, *5*, 380–390. [[CrossRef](#)] [[PubMed](#)]
34. Spitale, F.M.; Vicario, N.; Rosa, M.D.; Tibullo, D.; Vecchio, M.; Gulino, R.; Parenti, R. Increased Expression of Connexin 43 in a Mouse Model of Spinal Motoneuronal Loss. *Aging* **2020**, *12*, 12598–12608. [[CrossRef](#)]
35. Yousef, H.; Morgenthaler, A.; Schlesinger, C.; Bugaj, L.; Conboy, I.M.; Schaffer, D.V. Age-Associated Increase in BMP Signaling Inhibits Hippocampal Neurogenesis. *Stem Cells* **2015**, *33*, 1577–1588. [[CrossRef](#)] [[PubMed](#)]
36. Armenteros, T.; Andreu, Z.; Hortigüela, R.; Lie, D.C.; Mira, H. BMP and WNT Signalling Cooperate through LEF1 in the Neuronal Specification of Adult Hippocampal Neural Stem and Progenitor Cells. *Sci. Rep.* **2018**, *8*, 9241. [[CrossRef](#)]
37. Sarkar, S.; Mirzaei, R.; Zemp, F.J.; Wei, W.; Senger, D.L.; Robbins, S.M.; Yong, V.W. Activation of NOTCH Signaling by Tenascin-C Promotes Growth of Human Brain Tumor-Initiating Cells. *Cancer Res.* **2017**, *77*, 3231–3243. [[CrossRef](#)]
38. Bond, A.M.; Peng, C.-Y.; Meyers, E.A.; McGuire, T.; Ewaleifoh, O.; Kessler, J.A. BMP Signaling Regulates the Tempo of Adult Hippocampal Progenitor Maturation at Multiple Stages of the Lineage. *Stem Cells* **2014**, *32*, 2201–2214. [[CrossRef](#)]
39. Shruster, A.; Ben-Zur, T.; Melamed, E.; Offen, D. Wnt Signaling Enhances Neurogenesis and Improves Neurological Function after Focal Ischemic Injury. *PLoS ONE* **2012**, *7*, e40843. [[CrossRef](#)] [[PubMed](#)]

**Disclaimer/Publisher’s Note:** The statements, opinions and data contained in all publications are solely those of the individual author(s) and contributor(s) and not of MDPI and/or the editor(s). MDPI and/or the editor(s) disclaim responsibility for any injury to people or property resulting from any ideas, methods, instructions or products referred to in the content.